

Structural monitoring of concrete segmental lining tunnels during construction with conventional and fibre optic instrumentation

Saleta Gil Lorenzo¹, Mohammed Elshafie², Kenichi Soga³, Robert J. Mair⁴, Peter Wright⁵,
Martin Clegg⁶

^{1, 2, 3, 4} University of Cambridge, Cambridge, UK

⁵ CH2MHill, London, UK

⁶ Geosense Ltd., Cambridge, UK

ABSTRACT: Cambridge University, in collaboration with Hochtief (UK) Construction and Crossrail Ltd., has instrumented four rings in the newly constructed Thames tunnel. This has provided a complete set of in-situ monitoring data on ring deformations collected by both conventional instrumentation and embedded distributed fibre optic strain sensing (DFOS). The monitoring regime was purposely designed to collect measurements during the construction process, including tunnelling and cross passage construction. The results will be used in the future to describe the real history of deformations with the view of enhancing the understanding of concrete segmental lining performance during construction and operation for shallow tunnels in chalk.

In this paper, the Thames tunnel field trials are briefly described and an example of strain measurements captured in one of the instrumented segments is discussed. Temperature compensation of actual strains is validated for concrete segmental linings with a universal ring configuration and some interesting aspects of the segment strain history during tunnelling are highlighted. A more thorough analysis and comprehensive set of field instrumentation data from embedded DFOS, vibrating wire strain gauges (VWSG), tilt meters and laser scanner will be published elsewhere in the future.

1 INTRODUCTION

Crossrail is a new 118 km railway line in the UK that connects central London with the west and east of Greater London, relieving London Underground from current and future excess demand in passenger volumes. Being one of Europe's largest infrastructure projects, it includes the construction of about 42 km of new tunnels, most of them in Central London. The Thames tunnel is the only tunnel in the Crossrail scheme that crosses the river Thames.

The 6.2 m internal diameter (ID) twin tunnels run from North Woolwich portal through Woolwich station box at the north side of the river and up to Plumstead portal at the south bank as shown in Figure 1. They are driven through chalk at a shallow depth, with an overburden height that varies from 12.8 m to about 20 m. The River Thames is subject to tides with fluctuations in water level of up to 7 m.



Figure 1. Plan view of Crossrail route and location of Thames tunnel.

The twin tunnels were excavated with a mix shield tunnel boring machine (TBM) running in slurry mode. The distance between the tunnels varies with the alignment, but at the areas of interest in the case study presented in this paper, the clearance is greater than two times the tunnel diameter, $2D$. The main tunnels are lined with a concrete segmental lining based on a tapered universal ring configuration. Each ring is made of seven segments and a wedge-shaped key stone. The nominal lining thickness is 300 mm, the segment width is 1.6 m and the length is about 2.8 m. The standard segments are steel fibre reinforced whilst the cross passage rings were designed with conventionally reinforced concrete segments. Steel fibres were included in the concrete mix of the cross passage segments to simplify logistics in the concrete plant.

An instrumentation monitoring scheme was agreed and funded by Crossrail, Hochtief (UK) Construction, CH2MHill and Cambridge University to capture the in situ response of four concrete segmental lining rings at several locations in the eastbound tunnel of the Thames tunnel. The field trials targeted the effect of construction activities such as tunnelling and cross passage construction adjacent to the instrumented rings. There has been significant research on tunnel stability, tunnelling-induced ground movements and the effect of these movements on adjacent structures, but only a limited amount of field monitoring data focuses on the performance of concrete segmental lining during construction, despite evidence suggesting that construction loads can govern the design of tunnel linings.

In this case study, several monitoring techniques were applied to (1) obtain a complete set of in-situ ring deformations, i.e. strain measurements in segments and joint rotations; and (2) validate the use of emerging technology in structural health monitoring (SHM), namely distributed fibre optic strain sensing (DFOS), for such complex structures subject to a variable loading history. Strains in segments were measured with both vibrating wire strain gauges (VWSG) and the Brillouin Optical Time Domain Reflectometry (BOTDR) technique for DFOS. Segment tilt to derive joint rotations was obtained from microelectromechanical (MEMS) biaxial tilt sensors installed in each of the instrumented segments. Laser scanning was also implemented after construction to (1) identify the deformed ring shape, and (2) measure joint rotations within the instrumented ring and offsets between adjacent segments.

The following section describes briefly the instrumentation layout and monitoring regime.

2 INSTRUMENTATION LAYOUT

Each segment of the instrumented rings, except for the key stone, was equipped with embedded distributed fibre optic strain and temperature sensors to capture total strains and temperature changes. A length of 30m of reinforced Fujikura fibre optic cable (single mode Fujikura 4-core

9.5/125 JBT-03813) was attached to the reinforcement cage of each segment. A unitube gel-filled loose cable (single mode Excel –core 9/125 OS1) was also installed as a dummy temperature cable to enable temperature compensation during data processing. The topology is shown in Figure 2. Two central loops were installed, in the hoop and longitudinal directions, both at the extrados (outer face) and intrados (inner face) of the instrumented sections; these measurements were intended to derive the distribution of average strain and curvature and hence axial forces and bending moments. Two additional loops in the hoop direction were included at the sides of the segment to complete the study and capture side effects within the segmental units. The optical cables were terminated at two stainless steel box-outs embedded in the segments to protect them during the segment casting.

Five VWS-2100 strain gauges were embedded in each instrumented segment, two pairs at the center of the segment in hoop and longitudinal directions, each pair with a strain gauge at the extrados and another at the intrados of the segment. The remaining strain gauge was placed at one side of the segment and oriented in longitudinal direction. Due to logistics and time constraints during the installation works, the strain gauges were offset from the central loop of the fibre optic sensors. The VWSGs were connected to a DT2055 ten channel data logger (RST instruments), which was housed at one of the embedded box-outs.

Finally, a MEMS tilt sensor and logger was fastened to the base of the second box-out with a mounting bracket and four concrete anchors.

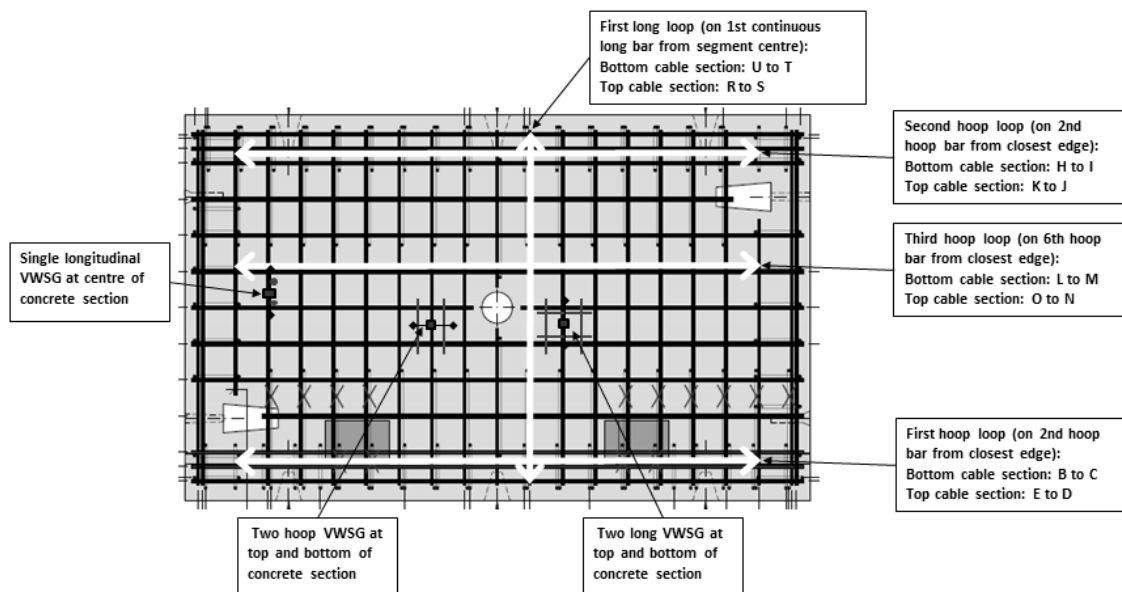


Figure 2. Instrumentation topology and location of box-outs in a precast concrete segment.

3 MONITORING REGIME

During segment casting, the VWSG data loggers were programmed to collect strain data at intervals of less than a minute, to monitor the casting and curing process and record any damage to the strain gauges that could have occurred especially during vibration of the segment moulds. At the segment yard, fibre optic strain readings were taken for each single segment, which were then used as baselines for future measurements in the tunnel, given that the segments were

subject to minimal loading at this stage. The VWSG and tilt loggers were programmed to start collecting data at regular intervals prior to the estimated ring erection date.

After ring erection, several measurements were performed during the installation activities to validate the integrity of the optical sensors, connectors and splices. BOTDR data was collected once the installation works were completed prior and during the following advance, and during the assembly of the subsequent ring. From this point onwards, continuous readings, every 30min or 1h, were set up to capture strains during the TBM passage. Tilt and VWSG loggers continued collecting data, initially at 15 min interval and 1h after some days passed the ring erection date until the end of 2014 when the installation was dismantled.

4 RESULTS AND DISCUSSION

The strain history at the center of segment KR4 is presented and discussed in this paper. Segment KR4 is placed at the crown of instrumented ring no. 4. Figure 3 show the strain increments developed with time in both hoop and longitudinal directions for the first 26 hours after ring erection. The strain values are relative to the BOTDR baseline readings and time zero refers to the completion of the instrumented ring erection. The BOTDR data included in Figure 3d was extracted from 150mm sections of the DFOS central hoop loop adjacent to the central pair of hoop strain gauges. The cylinder thrust applied onto segment KR4 for the first six TBM advances is also illustrated for comparison.

Strain measurements are a good performance indicator for SHM of precast operational structures as long as thermal effects and creep deformations can be delimited and mechanical strains derived. The compressive and tensile mechanical strains at peak stresses, bounding plastic behavior and cracking in concrete, remain roughly constant for a wide variety of concrete grades (Eurocode 2004).

Creep deformations developed with time may be of the same order as instantaneous strains, and are not fully recoverable (Neville & Brooks, 2010). Therefore the identification of the creep component in concrete deformations is valuable. In this line, the first author carried out some creep tests on concrete samples subjected to a similar history of environmental conditions and loaded at the age when the instrumented segments were assembled in the tunnel. These tests are out of the scope of this paper. With regard to thermal effects in concrete segmental linings, the adequacy of temperature compensated strains is discussed in the following subsection.

Strain sensors affected by temperature changes provide measurements of apparent strain, which is the result of the total strain experienced by the measurand, i.e. the actual strain, and the sensitivity of the sensor, e.g. thermally-induced frequency shift in the BOTDR technique or thermal expansion or contraction of the VWSG steel wire. The temperature effects related to the strain sensor can be corrected by determining thermal fluctuations with a thermistor (VWSG) or dummy temperature optical cable (BOTDR) if the sensor temperature coefficients, under constant strain, are known.

4.1 *Temperature compensation*

In tunnels, temperature variations tend to be small compared to other structures such as bridges except during the tunneling stage. Heat is mainly generated by friction between the cutter head and the ground as the tunnel boring machine (TBM) advances and by curing of the annular grout, leading to a temperature increase of about 15°C in the segments for this case study. Depending on their boundary conditions, the thermally-induced component of the total strains

could range from $0\mu\epsilon$, in the case of full restraint, up to $150\mu\epsilon$ for free expansion or contraction. Considering the values of total strains captured in the field trials, temperature compensation becomes a key aspect in the correct interpretation of strain data.

Temperature compensation assumes that thermally-induced strains in the measurand structure are not restricted, and as such, the total value of thermal strains developed for a given temperature increment is subtracted from the actual strains to obtain the mechanical strains in the structure. Concrete segmental linings are hyperstatic structures and therefore partial or total restraints could be imposed at the boundary of the segmental units, invalidating the application of temperature compensation.

The temperature distribution within a ring cross-section is approximately uniform over time. Since the coefficient of thermal expansion of the bolts between ring segments ($12.2\mu\epsilon/^\circ\text{C}$ for steel) is higher than that of concrete ($10.5\mu\epsilon/^\circ\text{C}$), each segment of the universal ring will be allowed to thermally expand or contract freely as a simply supported curved beam.

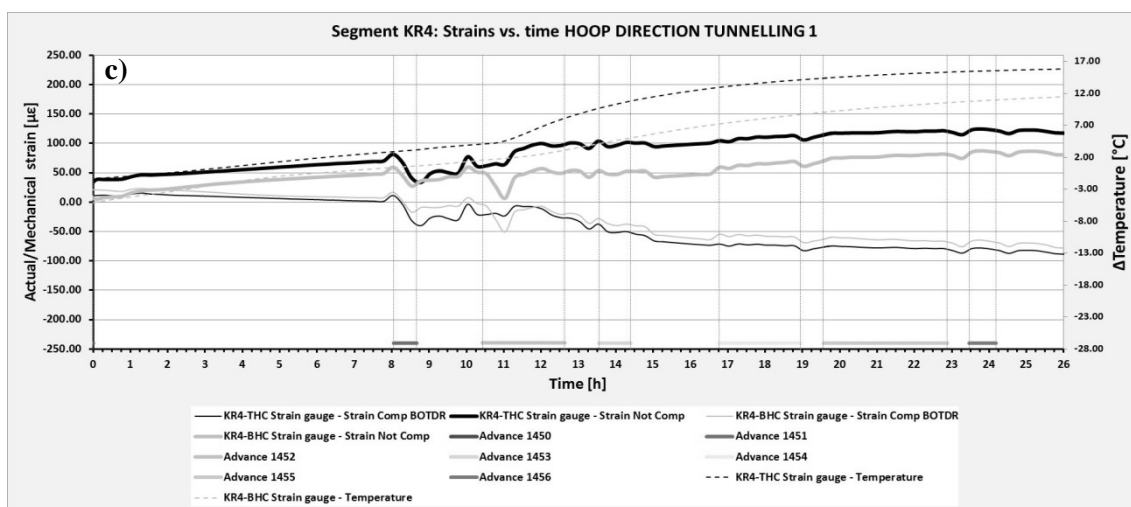
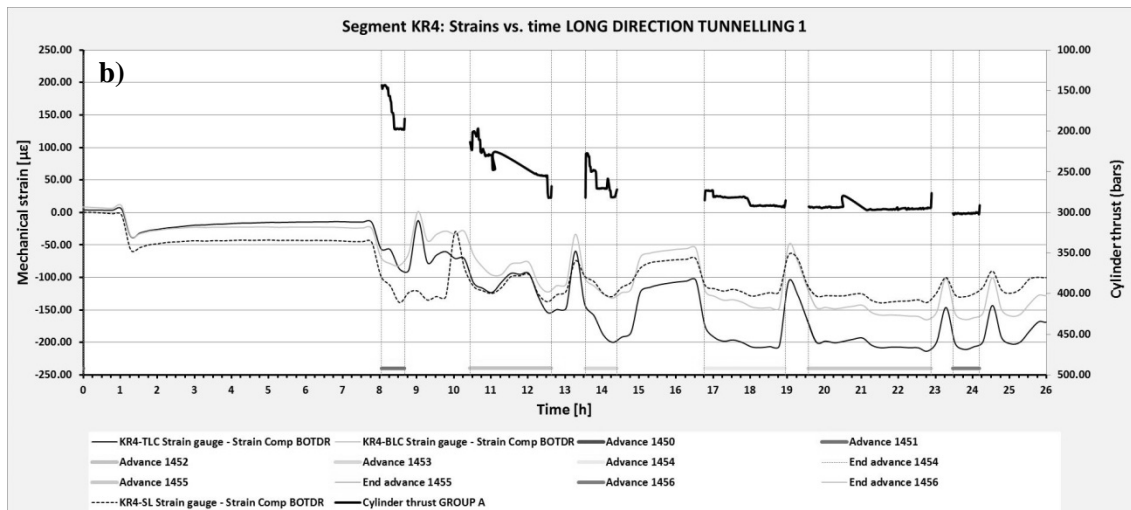
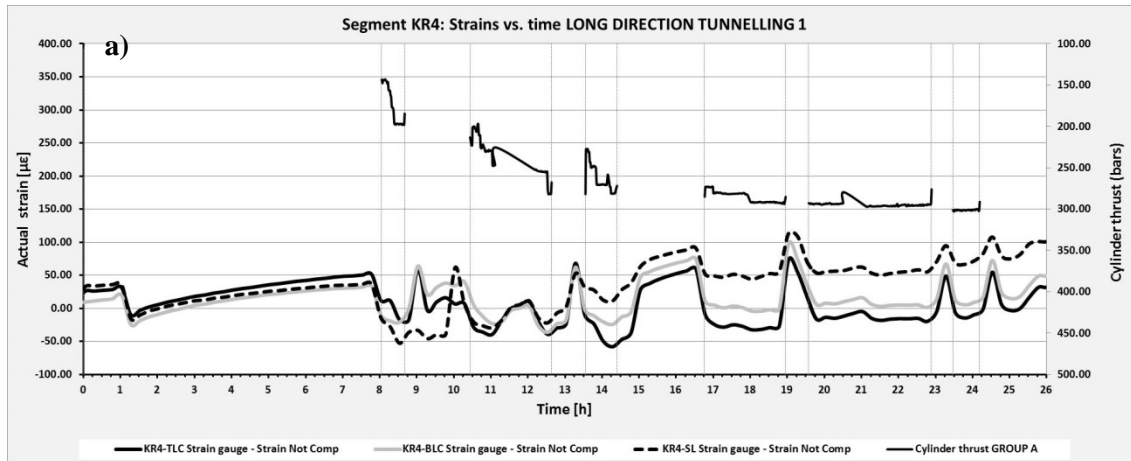
The profile of temperature increments along the tunnel axis, or over time, shows a smooth temperature increase from the last ring installed in the tunnel onwards, which remains constant after the following six rings. Gradients become significant only once the ring is outside the tail skin and hydration of the cementitious grout around the particular ring is initiated. For these reasons, the assumption of unrestrained thermal strains in the hoop direction could be justified.

In the longitudinal direction, the concrete segments and packers at the back of the tail skin will be exposed to the temperature profile described above. The thermal expansion of these rings could be absorbed by the lining structure behind them as demonstrated by a quick calculation based on a spring system of two parallel springs fixed at opposite ends. The first spring would represent the expansive concrete segment, and the second spring the sequence of several segments and packers behind. Considering the elastic response of a row of, for example, ten segments, and packers, with Young moduli of 38GPa and 3.5GPa respectively, the thermal strain induced by a 15°C temperature increase in a concrete segment could develop freely in more than 90% of the value in unrestrained conditions. This would validate the use of temperature compensated strains as representative of mechanical strains in the longitudinal direction.

Differential strains across the segment thickness due to a temperature gradient between extrados and intrados of the segments could be accommodated by slight rotations of the convex-to-convex longitudinal joints in hoop and additional axial deformations of the structural components in previous rings.

The comparison between the history of cylinder thrust acting on segment KR4 during the TBM advance and actual and temperature compensated longitudinal strains experienced by the segment supports the explanation above. Figure 3b shows that there is good agreement between gradients of temperature compensated strains and cylinder thrust for each of the TBM advances and, overall, for the first 26 hours of ring life. Conversely, actual longitudinal tensile strains in Figure 3a increase with time despite ram loads being of greater magnitude, as they are affected by a comparatively substantial temperature rise.

In addition, actual strains, hoop and longitudinal, are tensile for most of the initial stages after ring erection, which could not be explained if thermally-induced strains were fully restrained – shown in Figures 3c and 3d. Temperature compensated hoop strains result in compressive values which, after 24 hours tend towards the hoop strains expected to develop due to earth and water pressures.



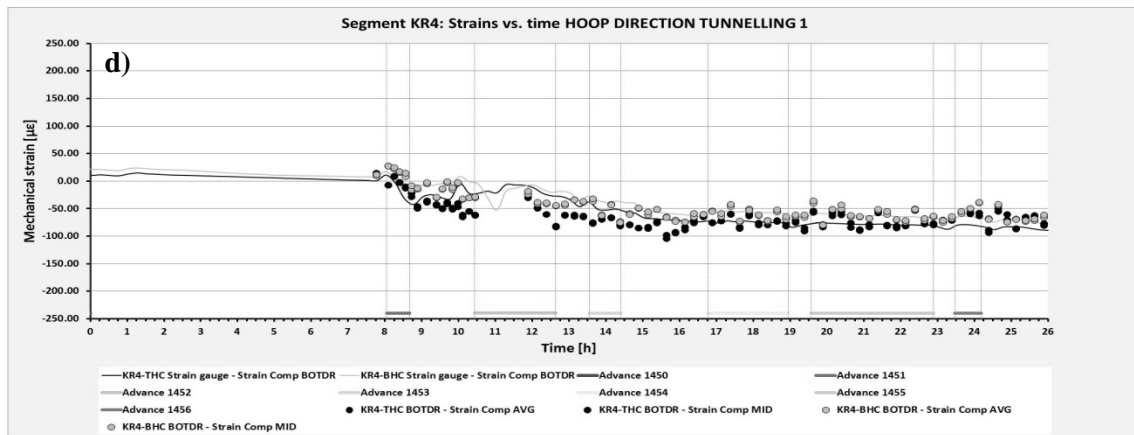


Figure 3. Strain history of segment KR4 centre for the first 26h after ring erection: a) Actual longitudinal strains (VWSG) and cylinder thrust; b) Mechanical longitudinal strains (VWSG) and cylinder thrust; c) Actual and mechanical hoop strains and temperature from VWSG; d) Mechanical hoop strains (BOTDR and VWSG).

4.2 Strain history

Only the initial stages in the strain history of the center of one segment (KR4) are briefly described in this paper. The discussion is drawn on temperature compensated strains.

When the first TBM advance after ring erection is initiated, segment KR4 is compressed as the hydraulic jacks push backwards onto the instrumented ring to propel the TBM forward. The strain distribution within the segment is not uniform, although the strain increments detected by the longitudinal VWSG at different positions range only from $45\mu\epsilon$ to $60\mu\epsilon$ in compression. At the same time, a tensile peak strain develops in the hoop direction corresponding to about a $10\mu\epsilon$ increment in tension. At this stage, the instrumented ring is still within the tail skin and the longitudinal joints are probably not fully closed yet. The ring experiences a tendency to expand radially when compressed axially due to the Poisson effect. Hoop tension calculated from the compressive strains experienced in hoop by the segment and the Poisson coefficient of concrete, 0.2, result in values approaching the $10\mu\epsilon$ measured by both DFOS and VWSG.

The ring emerges from the shield tail after the TBM has advanced for about half the width of a segment. At this point, seal and grout pressures start acting on the ring and govern hoop strains. The longitudinal joints close and hoop compression develops in the segment center. Compression increases progressively as the TBM advances and the annular grout hardens, creating a bonding interface between the lining and the ground. Water and earth pressures can now be effectively transferred to the lining. The mechanical compressive strains are around $75\mu\epsilon$ after one day in the ring life and bending is not significant in the hoop direction. These results are consistent with partial overburden acting on the ring and with the structural behavior of a concrete segmental ring provided with convex-to-convex joints.

Regarding the longitudinal direction, there is a good correlation between longitudinal strains and cylinder thrust applied to the segment as measured by the TBM systems. Some examples are tabulated below, where significant or sudden changes in cylinder thrust during TBM advance are compared to measured or calculated strain increments in the longitudinal direction. The calculated strains are obtained by applying a correction factor, F_c , taken as the ratio of the total area of the ram pads acting on the segment and the total side area of the segment.

Table 1. Cylinder thrust increments versus measured and calculated longitudinal strain increments

Advance	Δ Thrust (bars)	$\Delta\varepsilon_{\text{long,meas}}$ ($\mu\varepsilon$)	$\Delta\varepsilon_{\text{long,calculated}}$ ($\mu\varepsilon$)
1 st (1451)	50	40	43
2 nd (1452)	60	50	52
4 th (1454)	15	10	13

Finally, it is also noticeable that longitudinal bending increases with time, especially from the second advance, advance 1452, reaching a peak at the fourth advance, advance 1454, and reducing slightly afterwards. This sagging moment could be the result of the ring floating upwards before grout hardening and the ring being bedded into the ground, as it is not experienced in the first two advances of the ring life.

5 CONCLUSIONS

Four universal rings were instrumented with conventional instrumentation and embedded distributed fibre optic strain sensing technology in the newly constructed Thames tunnel. A complete set of in-situ ring deformations, i.e. strain measurements in segments and joint rotations, were collected during the construction stages, including tunneling and cross passage construction.

The early history of strains recorded at the center of a crown segment after ring erection with embedded DFOS and VWGS is presented and briefly discussed in this paper. A more thorough analysis and comprehensive set of field instrumentation data from embedded DFOS, VWGS, tilt meters and laser scanner will be published elsewhere in the future.

Temperature compensation of actual strains is validated for concrete segmental linings with a universal ring configuration. Hypotheses are proposed and corroborated by the examination of actual strains, temperature compensated strains and the cylinder thrust applied onto the segment over time.

The temperature compensated strain measurements evidence the development of tensile hoop strains due to the Poisson effect caused by the action of the hydraulic jacks onto the segment. Hoop compression grows gradually as the instrumented ring emerges from the tail skin and values are consistent with expected earth and water pressures. A good correlation was observed between the cylinder thrust and longitudinal strains over time and the progressive sagging moments in axial direction may suggest floating being experienced by the ring.

6 REFERENCES

- Neville, AM, and Brooks, JJ. 2010, 'Concrete technology', 2nd edition, Pearson Education Ltd, Essex, UK.
- BS EN 1992-1-1: 2004, 'Eurocode 2: Design of concrete structures – Part 1-1: General rules and rules for buildings', Incorporating corrigendum January 2008 and November 2010, BSI, London, UK.